International Journal of Civil Engineering

Structure Steel

Efficient finite element analysis using graph-theoretical force method; tetrahedron elements

A. Kaveh[1,*], M.S. Massoudi[2]

Received: April 2014, Revised: May 2014, Accepted: June 2014

Abstract

Formation of a suitable null basis is the main problem of finite elements analysis via force method. For an optimal analysis, the selected null basis matrices should be sparse and banded corresponding to sparse, banded and well-conditioned flexibility matrices. In this paper, an efficient method is developed for the formation of the null bases of finite element models (FEMs) consisting of tetrahedron elements, corresponding to highly sparse and banded flexibility matrices. This is achieved by associating special graphs with the FEM and selecting appropriate subgraphs and forming the self-equilibrating systems (SESs) on these subgraphs. Two examples are presented to illustrate the simplicity and effectiveness of the presented graph-algebraic method.

Keywords: *Three dimensional elements, Tetrahedron elements, Higher order elements, Finite element method, Force method, Null basis matrix, Flexibility matrix, Graph Theory.*

1. Introduction

The force method of structural analysis in which the member forces are used as unknowns is appealing to engineers since the properties of members of a structure most often depend on the member forces rather than joint displacements. This method was used extensively until 1960. The advent of the digital computer and the amenability of the displacement method for computation attracted most researchers. As a result, the force method and some of the advantages it offers in optimization and non-linear analysis and optimization has been neglected.

Five different approaches are adopted for the force method of structural analysis, classified as: Topological force methods, Graph theoretical methods, Algebraic force methods, Mixed algebraic-combinatorial force methods, and Integrated force method.

Topological methods have been developed by Henderson [1] Maunder [2] and Henderson and Maunder [3] for rigid-jointed skeletal structures. Graph theoretical methods based on cycle bases of the graph models are due to Kaveh [4-5]. These methods are generalized to cover different types of skeletal structures such as rigid-jointed frames, pin-jointed planar trusses and ball-jointed space trusses in [6-7].

Algebraic methods have been developed by Denke [8], Robinson [9], Topçu [10], Kaneko et al. [11], and Soyer and Topçu [12]. Mixed algebraic-topological methods have been used by Gilbert et al. [13] Coleman and Pothen [14-15], Pothen [16], and Heath et al. [17]. The integrated force method has been developed by Patnaik [18-19], in which the equilibrium and compatibility conditions are satisfied simultaneously in terms of the element force variables.

Recently applications of the graph theory methods are extended to two classes of finite element models. The first class takes the element forces along the edges of the elements [20-25] and in the second class the element forces are concentrated at the mid-edge of the edges of the elements [26].

In this paper, an efficient method is developed for the formation of null bases for finite element models comprising of tetrahedron elements leading to highly sparse and banded flexibility matrices, and can be used for optimal finite element analysis by the force method. This is achieved by associating a special graph to the finite element model and selecting subgraphs (known as γ-cycles [6]) for the formation of localized self-equilibrating stress systems (null vectors). Their numerical values are calculated by an algebraic process. The efficiency and accuracy of the present method is illustrated through simple examples.

** Corresponding author: alikaveh@iust.ac.ir*

1 Professor, Centre of Excellence for Fundamental Studies in Structural Engineering, Iran University of Science and Technology, Narmak, Tehran-16, Iran

2 PhD Student, School of Civil Engineering, Iran University of Science and Technology, Narmak, Tehran-16, Iran

2. Formulation of Force Method

Consider a discrete or discretized structure which is statically indeterminate. The *m*-dimensional vector ***r*** contains independent element (member) forces, and an *n*-dimensional vector ***p*** denotes the nodal loads. The equilibrium equations of the structure can then be expressed as:

$$\mathbf{Ar} = \mathbf{p} \tag{1}$$

where ***A*** is an *n*×*m* equilibrium matrix. Assuming stability for the structure, the equilibrium matrix will have full rank, i.e. $t = m - n > 0,\ rank(\mathbf{A}) = n$.

Also the member forces can be written as the sum of the particular and complementary solutions, where ***q*** is the *t*-dimensional vector of the redundant forces.

$$\mathbf{r} = \mathbf{B}_0\mathbf{p} + \mathbf{B}_1\mathbf{q} \tag{2}$$

$\boldsymbol{B}_0$ and $\boldsymbol{B}_1$ have *m* rows and *n*, and *t* columns, respectively. Pre-multiplying both sides of Eq. (2) by ***A*** and using Eq. (1) lead to

$$\mathbf{AB}_0 = \mathbf{I} \tag{3}$$

$$\mathbf{AB}_1 = \mathbf{0} \tag{4}$$

Here, $\boldsymbol{B}_0$ and $\boldsymbol{B}_1$ are not unique for a structure and many of such matrices can be formed. $\boldsymbol{B}_1$ is called static basis or self-stress matrix. This basis is known as null basis in mathematics and each column of the null basis matrix is known as a null vector. The null space and null vectors are mathematical counterparts of the complementary solution space and self-equilibrating systems, respectively.

Minimizing the complementary potential energy subjected to the constraint as in Eq. (1) requires ***r*** to minimize the quadratic form

$$\min imize(\tfrac{1}{2}\mathbf{r}^t\mathbf{F}_m\mathbf{r}) \tag{5}$$

Here**,** $\boldsymbol{F_m}$ is a *m*×*m* block diagonal matrix known as the unassembled flexibility matrix containing the flexibility matrices of the elements of a structure in its block diagonal entries. Coupling Eq. (5) and Eq. (2) results in

$$\mathbf{q} = -(\mathbf{B}_1^t\mathbf{F}_m\mathbf{B}_1)^{-1}(\mathbf{B}_1^t\mathbf{F}_m\mathbf{B}_0)\mathbf{p} \tag{6}$$

According to Eq. (6) by solving a set of equations, redundant forces can be found.

After the determination of the member forces, using the load-displacement relationship for each member, one can write member distortion as

$$[\mathbf{u}] = [\mathbf{F}_m][\mathbf{r}] = [\mathbf{F}_m][\mathbf{B}_0 \quad \mathbf{B}_1]\begin{bmatrix}\mathbf{p}\\ \mathbf{q}\end{bmatrix} \tag{7}$$

Using virtual work, nodal displacements can be calculated as

$$[\mathbf{v}_0] = [\mathbf{B}_0^t][\mathbf{u}] \tag{8}$$

Combining Eq. (7) and Eq. (8) leads to

$$\mathbf{v}_0 = \mathbf{B}_0^t\mathbf{F}_m\mathbf{B}_0\mathbf{p} + \mathbf{B}_0^t\mathbf{F}_m\mathbf{B}_1\mathbf{q} \tag{9}$$

Substituting Eq. (6) in Eq. (9) and using $\mathbf{D}_{ij} = \mathbf{B}_i^t\mathbf{F}_m\mathbf{B}_j$ leads to

$$\mathbf{v}_0 = \left[\mathbf{D}_{00} - \mathbf{D}_{01}\mathbf{D}_{11}^{-1}\mathbf{D}_{10}\right]\mathbf{p} = \mathbf{Fp} \tag{10}$$

Therefore the overall flexibility matrix of structure is obtained as

$$\mathbf{F} = \mathbf{D}_{00} - \mathbf{D}_{01}\mathbf{D}_{11}^{-1}\mathbf{D}_{10} \tag{11}$$

For free vibration of linear structure without damping we have

$$[[\mathbf{K}] - \omega^2[\mathbf{M}]][\mathbf{v}_0] = \mathbf{0} \tag{12}$$

Obviously $\mathbf{Kv}_0 = \mathbf{p}$ and substituting Eq. (10) in Eq. (12) leads to

$$[[\mathbf{I}] - \omega^2[\mathbf{M}][\mathbf{F}]][\mathbf{p}] = \mathbf{0} \tag{13}$$

Then the frequency equation of the system in the force method is obtained as

$$|[\mathbf{M}][\mathbf{F}] - \lambda[\mathbf{I}]| = 0 \ \ and \ \ \lambda = 1/\omega^2 \tag{14}$$

Efficiency of this analysis depends on the required time for the formation of the matrix $\mathbf{G} = \mathbf{B}_1^t\mathbf{F}_m\mathbf{B}_1$ and its characteristics, i.e. sparsity and bandedness together with its conditioning. For the formation of a well-structured matrix ***G***, one should select a well-structured $\boldsymbol{B}_1$ matrix.

Many algebraic procedures based on various matrix factorizations such as Gauss-Jordan elimination, LU, QR, LQ exist for the formation a null basis matrix $\boldsymbol{B}_1$ of an equilibrium matrix ***A*** [13-17]. Basic concept of these methods is described briefly in the following. Let matrix ***A*** be partitioned using a column permutation matrix ***P*** as below:

$$\mathbf{AP} = [\mathbf{A}_1, \mathbf{A}_2] \tag{15}$$

Where $\boldsymbol{A}_1$ is a *n*×*n* non-singular matrix. Obviously matrix $\boldsymbol{B}_1$ can be written as

$$\mathbf{B}_1 = \mathbf{P}\begin{bmatrix} -\mathbf{A}_1^{-1}\mathbf{A}_2 \\ \mathbf{I} \end{bmatrix} \tag{16}$$

Turn-back method

This method is developed in [10-11] and it is briefly described in this section. We write the matrix $\boldsymbol{A}$= ($\boldsymbol{a}_1$, $\boldsymbol{a}_2$, $\boldsymbol{a}_3$,…,$\boldsymbol{a}_n$) by columns. A start column is a column such that the ranks of ($\boldsymbol{a}_1$, $\boldsymbol{a}_2$, $\boldsymbol{a}_3$,…, $\boldsymbol{a}_{s-1}$) and ($\boldsymbol{a}_1$, $\boldsymbol{a}_2$, $\boldsymbol{a}_3$,…, $\boldsymbol{a}_s$) are equal. Equivalently, $\boldsymbol{a}_s$ is a start column if it is linearly dependent on the lower-numbered columns. The coefficients of this linear dependency give a null vector whose highest numbered non-zero is in position s. It is easy to see that the number of start columns is $t = m - n$, which is the same as the dimension of the null space of $\boldsymbol{A}$.

The start column can be found by performing a QR factorization of $\boldsymbol{A}$, using orthogonal transformations to annihilate the sub-diagonal non-zeros. Suppose that in carrying out the QR factorization we do not perform column interchanges but simply skip over any columns that are already zero on and below the diagonal. The result will then be a factorization of the form

$$\boldsymbol{A} = \boldsymbol{Q}\begin{bmatrix} \boldsymbol{R} \\ \mathbf{0} \end{bmatrix} \tag{17}$$

The start columns are those columns where the upper triangular structure jogs to the right, that is, $\boldsymbol{a}_s$ is a start column if the highest non-zero position in column s of $\boldsymbol{R}$ is no larger than the highest non-zero position in earlier columns of $\boldsymbol{R}$.

The Turn-back method finds one null vector for each start column $\boldsymbol{a}_s$ by 'turning back' from column s to find the smallest k for which columns ($\boldsymbol{a}_s$, $\boldsymbol{a}_{s-1}$, $\boldsymbol{a}_{s-2}$,…, $\boldsymbol{a}_{s-k}$) are linearly dependent. The null vector has a non-zero only in position $s - k$ through s. Thus, if k is small for most of the start columns, then the null basis will have a small profile. Note that the Turn-back operates on $\boldsymbol{A}$, and not on $\boldsymbol{R}$. The initial QR factorization of $\boldsymbol{A}$ is used only to determine the start columns, and then discarded.

The null vector that Turn-back finds from start column $\boldsymbol{a}_s$ may not be non-zero in position s. Therefore, turn-back needs to have some way to guarantee that its null vectors are linearly independent. This can be accomplished by forbidding the left-most column of the dependency for each null vector from participating in any later dependencies. Thus, if the null vector for start column $\boldsymbol{a}_s$ has its first non-zero in position $s - k$, every null vector for a start column to the right of $\boldsymbol{a}_s$ will be zero in position $s - k$.

3. Independent Element Forces and Flexibility Matrix of Tetrahedron Elements

For the generation of the equilibrium matrix **A** of a FEM, a system of independent force systems should be defined and also their relations with the element nodal forces should be established [27].

In displacement method we have three forces at each node of the element. For an element with N nodes, $3 \times N$ nodal forces can be defined. Using six equilibrium equations, $3N - 6$ independent forces will be remained. In other words, there are $3N - 6$ independent element forces in an element with N nodes. The nodal forces and element forces systems are shown in Table 1 for tetrahedron elements with various numbers of boundary nodes. For the higher order elements, the element forces system can be obtained with the same procedure.

Table 1 The nodal forces and element forces systems for various tetrahedron elements.

Element	Number of Nodes	Size of $\boldsymbol{T}$	Nodal Forces $\boldsymbol{S}$	Elemental Forces $\boldsymbol{F}$	Element shape
Linear	4	4×6	$S_{12\times1} = [S_1..S_{12}]^t$	$F_{6\times1} = [F_1..F_6]^t$	
Quadratic	10	30×24	$S_{30\times1} = [S_1..S_{30}]^t$	$F_{24\times1} = [F_1..F_{24}]^t$	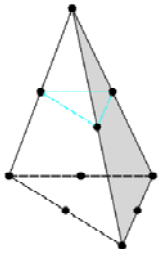

Cubic	20	60×54	$S_{60\times1}=[S_1..S_{60}]^t$	$F_{54\times1}=[F_1..F_{54}]^t$	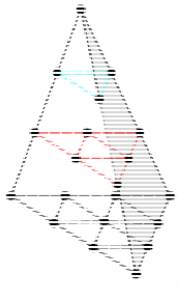
Quartic	35	105×99	$S_{105\times1}=[S_1..S_{105}]^t$	$F_{99\times1}=[F_1..F_{99}]^t$	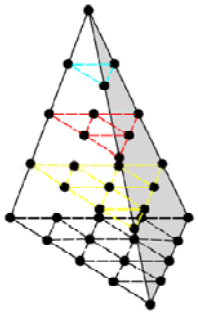

These element forces $\boldsymbol{F}$ can be related to the nodal forces $\boldsymbol{S}$ for a N-node element by a $(3N)\times(3N-6)$ transformation matrix using Eq. (18) as

$$\mathbf{S}=\mathbf{TF} \tag{18}$$

Transformation matrix can be formed simply as

$(n_1,n_2)=$ *end nodes of element force* F_j

For $i=1:N$

  For $j=1:3N-6$

    If $i==n_1$ $T(3i-2,j)=m_{n_1n_2}$ *and* $T(3i-1,j)=n_{n_1n_2}$ *and* $T(3i,j)=p_{n_1n_2}$

    If $i==n_2$ $T(3i-2,j)=m_{n_2n_1}$ *and* $T(3i-1,j)=n_{n_2n_1}$ *and* $T(3i,j)=p_{n_2n_1}$

  End

End

where x_i, y_i and z_i are the Cartesian coordinates of node i, $m_{ij}=\dfrac{x_i-x_j}{l_{ij}}$, $n_{ij}=\dfrac{y_i-y_j}{l_{ij}}$ and $p_{ij}=\dfrac{z_i-z_j}{l_{ij}}$ are the direction cosines and l_{ij} is the length of the line between nodes *i* and *j*.

Formulation of a discrete element equivalent to the actual continuous structure is the first step in matrix structural analysis. For a linear system it can be assumed that the stresses $\boldsymbol{\sigma}$ are related to the forces $\boldsymbol{F}$ by linear equation as

$$\boldsymbol{\sigma}=\bar{\mathbf{c}}\mathbf{F} \tag{19}$$

The matrix $\bar{\mathbf{c}}$ represents a statically equivalent stress system due to the unit force $\boldsymbol{F}$. The flexibility matrix of an element can be written as

$$\mathbf{f}_m=\int_V \bar{\mathbf{c}}^t\boldsymbol{\varphi}\bar{\mathbf{c}}dV \tag{20}$$

The integration is taken over the volume of the element, where $\boldsymbol{\varphi}$ is the matrix relating the stresses to strains $\boldsymbol{\varepsilon}=\boldsymbol{\varphi\sigma}$ in three dimensional problems. The primary step in the formation of the flexibility matrix of an element is determining the matrix $\bar{\mathbf{c}}$. It is obvious that the i^{th} column of $\bar{\mathbf{c}}$ represents the resultant stresses due to unit element force F_i in the force method and also stresses due to nodal forces S is equal to the i^{th} column of $\boldsymbol{T}$ utilizing the displacement method. Hence, we can form matrix $\bar{\mathbf{c}}$ using the stiffness properties of the tetrahedron element using the displacement method. Now the flexibility matrix of the element in the force method is formed from Eq. (20) using Gauss numerical integration method with eight Gauss points (2×2×2 Gauss Points Integration).

4. Graphs Associated with Finite Element Models

4.1. Basic graph theory definitions

A graph S consists of a set of elements, $N(S)$, called *nodes* and a set of elements, $M(S)$, called *members*, together with a relation of incidence which associates two distinct nodes with each member, known as its *ends*. Two nodes of a graph are called *adjacent* if these nodes are the end nodes of a member. A member is considered *incident* with a node if it is an end node of the member. The *degree* of a node is the number of members incident with that node. A *subgraph* S_i of a graph S is a graph for which $N(S_i) \subseteq N(S)$ and $M(S_i) \subseteq M(S)$, and each member of S_i has the same ends as in S. A *path* of S is a finite sequence $P_i = \{n_0, m_1, n_1, ..., m_p, n_p\}$ whose terms are alternately distinct nodes n_i and distinct members m_i of S for $1 \le i \le p$, and n_{i-1} and n_i are the two ends of m_i. Two nodes n_i and n_i are said to be *connected* in S if there exists a path between these nodes. A *cycle* is a path $(n_0, m_1, n_1,..., m_p, n_p)$ for which $n_0 = n_p$ and $p \ge 3$; i.e. a cycle is a closed path. The cycles of a graph form a vector space known as the *cycle space*. The dimension of this space for a connected graph S is known as the *first Betti number*, $b_1(S) = M(S)–N(S)+1$, of the graph, where $M(S)$ and $N(S)$ are the number of members and nodes of S, respectively. In order to transfer the topological property of a finite element model to the connectivity of a graph ten different graphs are introduced in [28-29].

4.2. An interface graph

The interface graph of a finite element model denoted by IG(FEM) can easily be constructed for tetrahedron FEM using the following rules:

1. This graph contains all the nodes of the FEM.
2. For each tetrahedron element of FEM, $3N-6$ graph members are associated. The edges of the interface graph will be numbered sequentially according to the patterns which were illustrated in Table 2. As was illustrated in Table. 2, there are some internal graph members in interface graph of a cubic, quartic or higher order tetrahedron element.

Table 2 Element forces and internal graph member for various tetrahedron members.

Element	shape	Element forces	Internal members
Linear		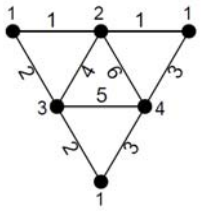	-
Quadatic	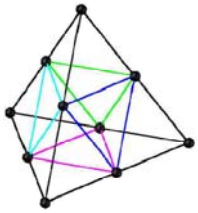	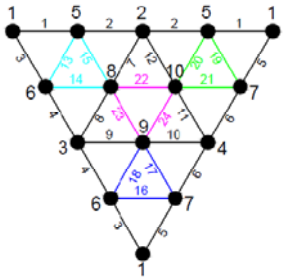	-
Cubic	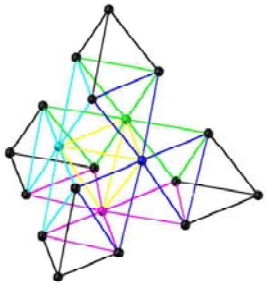	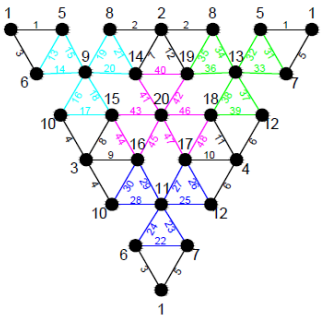	[9 ,13] [9 ,11] [11,13] [9 ,20] [11,20] [13,20]

Quartic	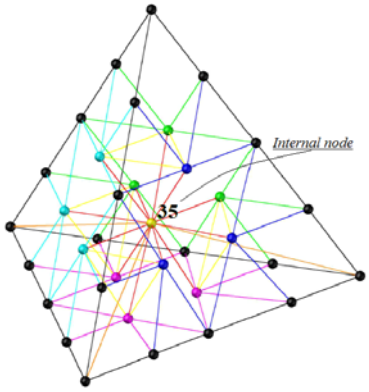	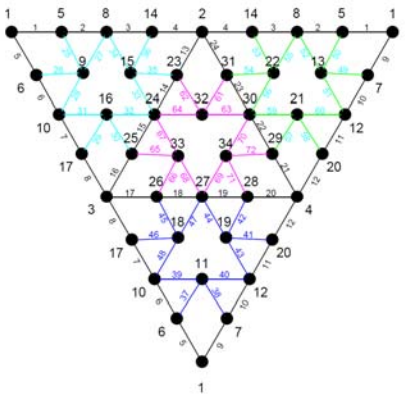	[9 ,11],[11,13] [13, 9],[16,18] [18,33],[33,16] [19,21],[21,34] [34,19],[15,32] [32,22],[15,22] [2 ,35],[3 ,35] [4 ,35],[9 ,35] [11,35],[13,35] [15,35],[16,35] [18,35],[19,35] [21,35],[22,35] [32,35],[33,35] [34,35]

4.3. Natural associate graph

The natural associate graph represented by NAG(FEM) is constructed by the following rules:

1. Nodes of the NAG(FEM) correspond to the elements of FEM.
2. For each pair of elements in FEM having specified number of common nodes, one member is added between the corresponding two nodes in NAG(FEM). The number of common nodes is dependent on the order of FEM elements. If two tetrahedron elements have these common nodes, they are adjacent or they have common side. According to Table 1, the number of common nodes for each type of element is as follow:

Element	Number of common nodes for two adjacent elements
Linear	3
Quadratic	6
Cubic	10
Quartic	15

NAG(FEM) can be constructed using the following procedure: One of the preliminary steps in FEA is defining the elements with their connected nodes. In this way the element connectivity matrix is constructed which contains the element-node incidence relationships. In the process of constructing the element connectivity matrix, another matrix which contains node-element incidence properties can be formed. This matrix is named the node connectivity matrix. Now using the element connectivity and the node connectivity matrices leads to an algorithm with complexity *O(n)* for an efficient generation of NAG.

In order to recognize the adjacent elements to the n^{th} element which have common nodes or one common face, first the connected nodes to the n^{th} element are identified from the element connectivity matrix. In the subsequent step using the node connectivity matrix, elements which have at least one common node with the n^{th} element are identified. Now it is convenient to seek for the adjacent elements in this reduced search space. A FEM with 24 tetrahedron elements and its corresponding NAG are illustrated in Fig. 1.

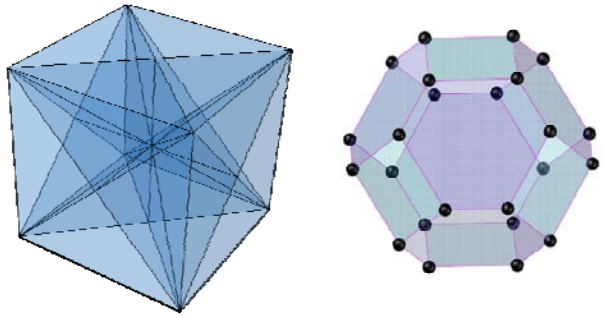

(a) (b)

Fig. 1 (a) Finite element model with 24 tetrahedron elements, (b) Natural associate graph (NAG)

4.4. Negative incidence number

Negative incidence number (NIN) is necessary for each node of NAG(FEM). This number can be found as following:

After generation of natural associate graph of the FEM, use an efficient method for its nodal numbering. A typical edge of the graph connects smaller number to the node with higher number. Negative incidence number of each node is the number of its adjacent nodes with smaller nodal number. Except the node numbered as 0, all the other nodes have one, two or three negatively incident edges defined as the negative incidence number of the node. Owing to the importance of these numbers in recognizing the types of SESs, the negative incidence numbers of the nodes of the graph should carefully be calculated. In Fig. 2, a tetrahedron FEM with element numbering, its corresponding associate graph and negative incidence number of nodes are shown. The nodes should be numbered such that the incidence numbers do not become large. Any simple nodal ordering will lead to a logical ordering.

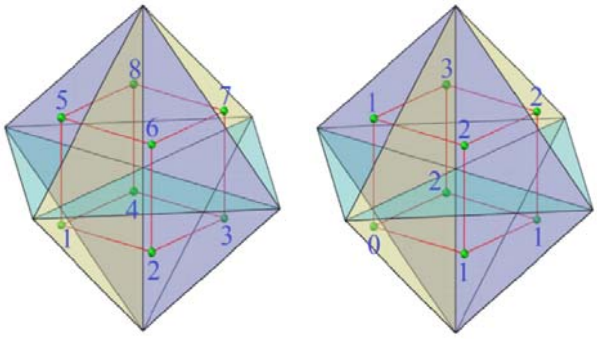

(a) (b)

Fig. 2 Finite element model with natural associate graph (red part); (a) nodal numbering of NAG; (b) negative incidence numbers of NAG

5. Pattern Corresponding to the Self-Equilibrating Systems

Considering Table 2, in order to find the patterns corresponding to the self-equilibrating systems, a tetrahedron element is simulated as a spatial truss formed as the 1-skeleton of the tetrahedron element together with some diagonal and internal members. This is possible since the independent element forces are applied in the nodes and are along the edges of the element. In Fig. 3, two interface graphs with four linear and quadratic elements are shown which are simulated as a spatial truss containing some multiple members.

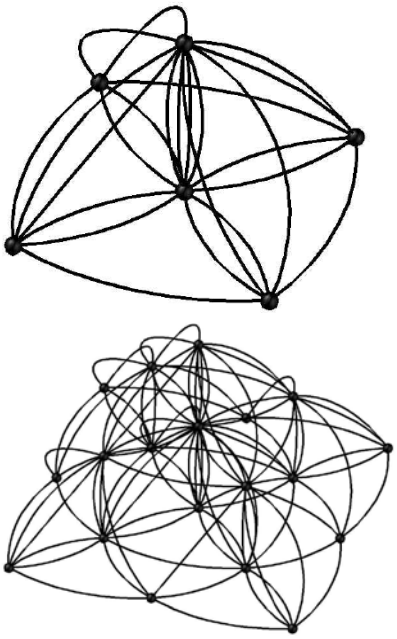

Fig. 3 (a) An IG(FEM) of four linear elements, b) An IG(FEM) of four quadratic elements

The statical indeterminacy of a spatial truss with m members and n nodes is given as $\gamma(S) = m - 3n + 6$; therefore, the degree of statical indeterminacy (DSI) of the entire model supported in a statically determinate manner can be calculated with the same relationship as

$$DSI = (3N - 6) \times M - 3n + 6 \tag{21}$$

where M is the total number of finite elements, N is the number of nodes of one element and n is the total number of nodes of the FEM.
With the above simulation, the patterns of the self-equilibrating systems can be identified as follows:

5.1. Type I self-equilibrating systems

For each k multiple member in equivalent truss model of FEM, there are k unknown forces and one equilibrium equation in the member's direction. Thus DSI of the substructure is equal to *k-1* and *k-1* self-equilibrating systems can be generated on each k multiple member of interface graph of the FEM. In this way, first each k multiple members are arranged in ascending order as (m_1, m_2, m_3,…, m_{k-1}, m_k) where ($m_1 < m_2 < m_3 <\ldots< m_{k-1} < m_k$). Each selection of two members from this list is valid to construct a type I self-equilibrating system, but in order to achieve a better bandwidth reduction; selection of adjacent members from the defined list is preferable. Therefore *k-1* duplicate members are selected as (m_1, m_2), (m_2, m_3),…, (m_{k-1}, m_k). Each pair (m_i, m_j) with $i < j$ represents the numbers of corresponding self-equilibrating system. The member with bigger number is selected as the generator of the current SES and also as a redundant force. The null vectors corresponding to the type I SESs have two non-zero entries in rows i and j equal to –1 and 1, respectively.

For FEMs with tetrahedron elements, more than 65% of the total self-stress systems are of Type I. Thus, a large percent of the minimal null vectors can be formed only by the determination of member numbers of these pairs. It should be noted that in the process of the formation of the interface graph, these pairs and their numbers can simply be identified.

5.2. Type II self-equilibrating systems

There are other types of self-equilibrating systems which are extracted from two adjacent elements of FEM. In other words, for two adjacent elements with N nodes, the *DSI* can be calculated as:

$$\begin{aligned} &DSI = (3N - 6) \times M - 3n + 6 \\ &\Rightarrow DSI = (3N - 6) \times 2 - 3 \times (2N - commonnodes) + 6 \end{aligned} \tag{22}$$

According to above equation, *DSI* of two adjacent elements for various orders can be obtained as demonstrated in Table 3. The number of SESs of Type I is the same as common member of adjacent element. Thus the number of remaining self-equilibrating systems is

$$Type\ II = DSI - Type\ I = \begin{cases} 0 & \rightarrow Linear\ element \\ 3 & \rightarrow Quadratic\ element \\ 9 & \rightarrow Cubic\ element \\ 15 & \rightarrow Quartic\ element \end{cases} \tag{23}$$

Table 3 The DSI, SESs of Type I and II of two adjacent elements.

Element	*N*	Common nodes	*n* *2N-common nodes*	*m* *2×(3N-6)*	*DSI* *m-3n+6*	Type I *common edges*	Type II
Linear	4	3	5	12	3	3	0
Quadratic	10	6	14	48	12	9	3
Cubic	20	10	30	108	24	15	9
Quartic	35	15	55	198	39	24	15

In other words, these SESs should be extracted from two adjacent elements. For example, the remaining subgraphs for two adjacent elements are shown in Fig. 4. After deleting the generators corresponding to type I SESs, the null vectors should be calculated from the remaining subgraph. These null vectors can easily be generated on the corresponding sub-structure utilizing an algebraic method. It should be noted that for linear elements, there is no SES of Type II.

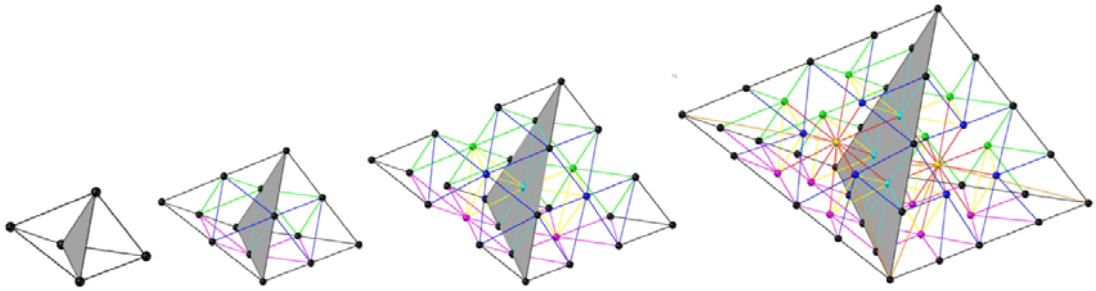

Fig. 4 Subgraph corresponding to SESs of type II

Apart from the aforementioned about generating the SESs of Type II, if there is at least a negative incidence number higher than one in a FEM, another important point should be considered which is explained below:

Some of the calculated SESs of Type II are not independent of the others. For example, for a FEM with four elements, four couple of adjacent elements can be recognized. The number of SESs of Type II can be obtained according to Eq. (23). It means that for each couple of two adjacent elements, 3, 9 or 15 SESs of Type II should be extracted. But, some of these SESs are dependent and should not be selected. For determining the independent SESs, an appropriate approach is proposed. In this approach, independent SESs will be recognized utilizing negative incidence number of elements and QR factorization method, simultaneously.

The SESs of Type II are extracted from two adjacent elements in a FEM which are the same as members of NAG(FEM). If a member of NAG(FEM) connects two elements M_i and M_j where $NIN_i > 1$ or $NIN_j > 1$, the independent SESs of Type II which can be extracted from the subgraph corresponding to these two adjacent elements can be recognized by QR factorization method.

The dependent SESs can be found by performing a QR factorization of $B_1 = [B_1^{Type\ I}, B_1^{Type\ II}]$, using orthogonal transformations to annihilate the sub-diagonal non-zeros where

$B_1^{Type\ I}$: all SESs of Type I

$B_1^{Type\ II}$: all independent SESs of Type II which are calculated up to now.

Suppose that in carrying out the QR factorization we do not perform column interchanges but simply skip over any columns that are already zero on and below the diagonal. The dependent SESs are those columns where the upper triangular structure jogs to the right, that is, column *s* is dependent SESs if the highest non-zero position in column *s* of ***R*** is no larger than the highest non-zero position in earlier columns of ***R***.

5.3. Type III self-equilibrating systems

Sub-structures which are topologically identical to the minimal cycles of the natural associate graph of FEM contain some type I, II and one or six type III self-equilibrating systems. In general, two types of minimal cycles can be extracted from the associate graph of an FEM. These cycles are as follows:

a) Type I minimal cycles of NAG(FEM)

In these cycles all the corresponding finite elements have at least two common nodes. Each cycle in this type passes through *M* finite elements as illustrated in Fig. 5.

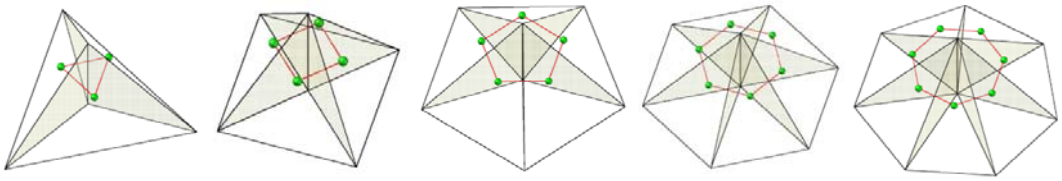

Fig. 5 Minimal cycles of NAG(FEM) pass through *M* finite elements which have at least two common nodes.

Corresponding interface graph of these *M* elements have *n* nodes and *m* edges for a FEM with *N* node elements which was calculated in Table 4. The DSI can be obtained, too.

By considering the SESs of Type I and II, the indeterminacy of remained subgraph is equal to 1 for all type of elements as

$$Type\ III = DSI - (Type\ I + Type\ II)$$

$$= \begin{cases} Linear & \rightarrow & (3M) - (3M-1) \\ Quadratic & \rightarrow & (12M-3) - ((9M-2) + (3M-2)) \\ Cubic & \rightarrow & (24M-6) - ((15M-2) + (9M-5)) \\ Quartic & \rightarrow & (39M-9) - ((24M-4) + (15M-6)) \end{cases} = \begin{cases} 1 \\ 1 \\ 1 \\ 1 \end{cases} \quad (24)$$

Thus, each Type I cycle corresponds to one null vector and the numerical values are calculated utilizing an algebraic method.

Table 4 Calculation of Type I cycle of NAG

Element	*m* Number of members	*n* Number of Nodes	*DSI* ($m-3n+6$)	Type I SESs	Type II SESs	Type III SESs (*DSI* – Type I – Type II)
Linear	M×6	M×4 - M×3 + 2	3M	3M-1	0	1
Quadratic	M×24	M×10 - M×6 + 3	12M-3	9M-2	3M-2	1
Cubic	M×54	M×20 - M×10 + 4	24M-6	15M-2	9M-5	1
Quartic	M×99	M×35 - M×15 + 5	39M-9	24M-4	15M-6	1

It should be noted that all the null vectors corresponding to cycles cannot be used in the formation of the final null basis. In other words, some of these SESs are dependent and should be selected and ignored. Here, QR factorization method should be applied to recognize dependent vectors.

b) Type II minimal cycles of NAG(FEM)

Each minimal cycle that surrounds an opening is called the type II minimal cycle. For example, consider Fig. 6. In this figure, a cube is divided in to five tetrahedron elements. Using twelve cubes or sixty tetrahedron elements, an opening with its NAG is generated. In this NAG there is a minimal cycle of type II.

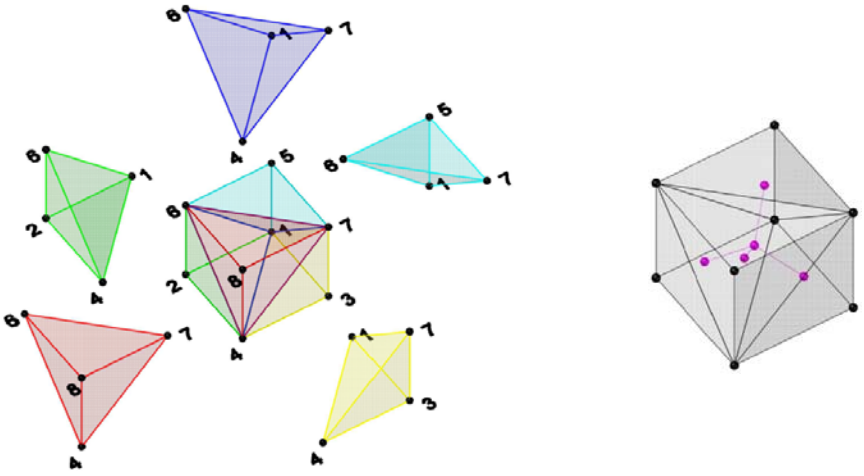

(a) (b)

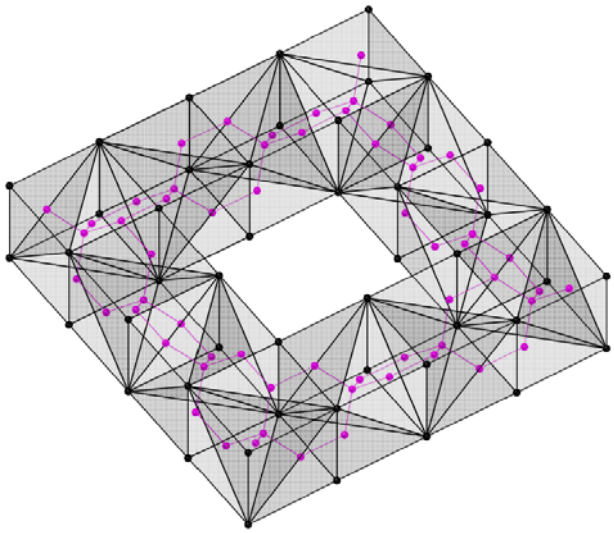

(c)

Fig. 6 (a) A cube comprising of five tetrahedron elements, (b) NAG of a cube, (c)A FEM with sixty tetrahedron elements conclude a minimal cycle of type II and its NAG

Such a cycle passes through M' finite elements and its corresponding interface graph has $(N-\text{common nodes})\times M'$ nodes and $M'\times(3N-6)$ members. The *DSI* of subgraph is

$$DSI = M'\times(3N-6) - 3\times(N-\text{common nodes})\times M' + 6$$

$$\Rightarrow \left.\begin{array}{rcll} linear & \rightarrow & N=4 & \text{common nodes}=3 \\ Quadratic & \rightarrow & N=10 & \text{common nodes}=6 \\ Cubic & \rightarrow & N=20 & \text{common nodes}=10 \\ Quartic & \rightarrow & N=35 & \text{common nodes}=15 \end{array}\right\} \Rightarrow DSI = \begin{cases} 3M'+6 \\ 12M'+6 \\ 24M'+6 \\ 39M'+6 \end{cases} \tag{25}$$

and $M'\times \underbrace{\begin{array}{l} linear \rightarrow 3 \\ Quadratic \rightarrow 9 \\ Cubic \rightarrow 15 \\ Quartic \rightarrow 24 \end{array}}_{\substack{\text{number of members} \\ \text{of common side of} \\ \text{two adjacent elements}}}$ SESs of type I and $M'\times \underbrace{\begin{array}{l} linear \rightarrow 0 \\ Quadratic \rightarrow 3 \\ Cubic \rightarrow 9 \\ Quartic \rightarrow 15 \end{array}}_{\substack{\text{number of SESs of Type II} \\ \text{between two adjacent elements}}}$ SESs of type II can be extracted.

The remaining SESs which can be extracted from interface graph corresponding to type II minimal cycle of NAG are

$$Type\ III = DSI - (type I\ \&\ II) = \left\{\begin{array}{l} linear \rightarrow 3M'+6 \\ Quadratic \rightarrow 12M'+6 \\ Cubic \rightarrow 24M'+6 \\ Quartic \rightarrow \underbrace{39M'+6}_{DSI} \end{array}\right\} - \left(\begin{array}{cc} 3M' & 0 \\ 9M' & 3M' \\ 15M' & 9M' \\ \underbrace{24M'}_{Type\ I} & \underbrace{15M'}_{Type\ II} \end{array}\right) = \begin{Bmatrix} 6 \\ 6 \\ 6 \\ 6 \end{Bmatrix} \tag{26}$$

Therefore, each type II minimal cycle corresponds to six null vectors which are calculated utilizing an algebraic method.

6. Selection of Generators

The most important point in type II and type III self-equilibrating systems is to select appropriate generators, because by eliminating these generators from IG(FEM), the sub-structure of primary structure of the IG(FEM) must remain stable. To achieve this, the following rule for appropriate selection of generators of type II SESs is suggested.

In each SES of type I, the member with bigger number is selected as the generator of the current SES and also as a redundant force. By now, in each subgraph corresponding

to Type II and type III SESs, those members are selected as the generators which have three properties as follows:

1. The candidate member was not selected as generator of previous SESs of any types.
2. By deleting the selected member, the remained subgraph will be stable.
3. The selected member has non-zero entries in an independent null vector.

7. Algorithm

Step 1: Generate the associate graph of the FEM and use an efficient method for its nodal numbering [26]. It is obvious that good numbering of this graph corresponds to good numbering of elements of the FEM. This numbering leads to a banded adjacency matrix of the graph and correspondingly to a banded flexibility matrix. Since numbering the members of the interface graphs corresponds to the element numbering of the finite elements, such a numbering is the only parameter for controlling the bandwidth of the flexibility matrix. Negative incidence number of the NAG(FEM) should be calculated in this step.

Step 2: Set up the equilibrium matrix of the FEM.

Step 3: Generate the interface graph and perform its numbering. The numbering of this graph should be performed according to the element numbering of the considered FEM. After this numbering the interface graph can easily be formed and its members can be numbered.

Step 4: Find the type I self-equilibrating systems. All multiple members of the interface graph are identified and the values −1 and 1 are assigned to appropriate rows (corresponding to the member numbers) and the corresponding minimal null vectors are created.

Step 5: Find the type II self-equilibrating systems. The SESs of type II should be extracted from two adjacent elements and independent ones should be selected among these SESs utilizing the approach which is explained in Sec.5.2. Calculate the corresponding null vectors from the relevant equilibrium sub-matrix in this step. Selection of generators should be done here.

Step 6: Find the type III self-equilibrating systems. For each minimal cycle of natural associate graph of FEM one or six SESs should be extracted as was described in Sec. 5.3. Calculate the corresponding null vectors from the relevant equilibrium sub-matrix and select their generators.

Step 7: Order the null vectors. At this step the constructed null vectors should be ordered such that their last non-zero entries form a list with an ascending order.

8. Numerical examples

In this section two FEMs are considered, which are assumed to be supported in statically determinate fashion. The equilibrium matrices are formed. Null bases and the flexibility matrices are constructed and the required computational times, and the condition numbers are calculated. In all the following examples, nz represents the number of non-zero entries and λmax/λmin is the ratio of the extreme eigenvalues taken as the condition number of a matrix. The comparison between present algorithm and algebraic force method will be shown in this section. Finally the present method is validated through comparison of analysis using the present graph-theoretical force method and the displacement method.

Example 1.

A thick beam-type structure supported in a statically determinate fashion is depicted in Fig. 7. The natural associate graph of FEM is illustrated in Fig. 8.This structure is discretized using 240 tetrahedron finite elements. The properties of the model are as follows:

Number of tetrahedron elements, M = 240 Elastic modulus, E = 2e+7 kN/m2 Poisson's ratio , ν = 0.2				
Number of nodes, N	Linear 205	Quadratic 1,053	Cubic 1,525	Quartic 3,321
DSI	1,131	4,167	8,391	13,803
Number of type I SESs	1,012	3,212	5,588	8,800
Number of type II SESs	0	836	2,684	4,884
Number of type III SESs	119	119	119	119

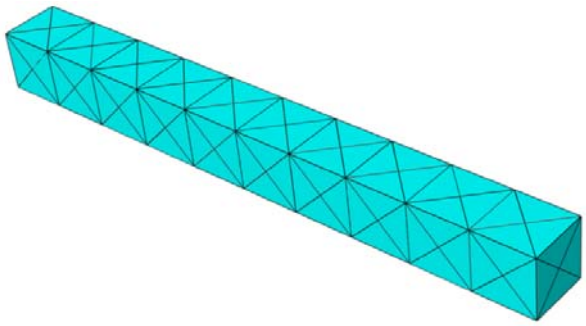

Fig. 7 A thick beam-type structure which is discretized using 240 tetrahedron elements

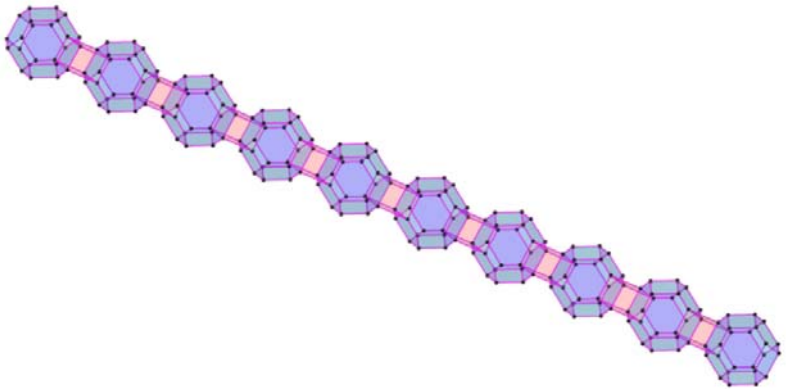

Fig. 8 Natural associate graph of FEM for thick beam-type structure of example 1

The pattern of equilibrium matrix is shown in Fig. 9 for various elements. The pattern of the final null basis obtained by the present method and LU factorization method are depicted in Fig. 10. The flexibility matrix (G) is also well-structured as shown in Fig. 11. The comparison between present method and LU factorization method is prepared in Table 5.

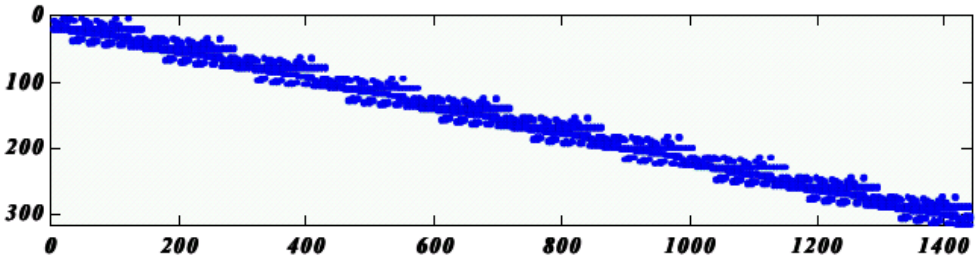

(a)

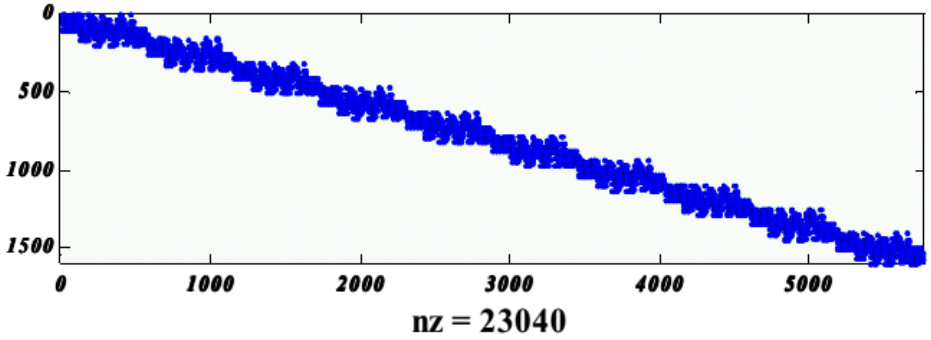

(b)

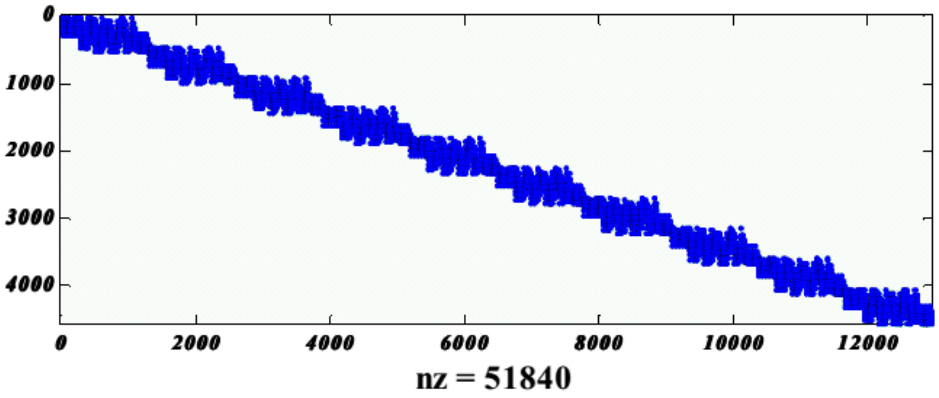

(c)

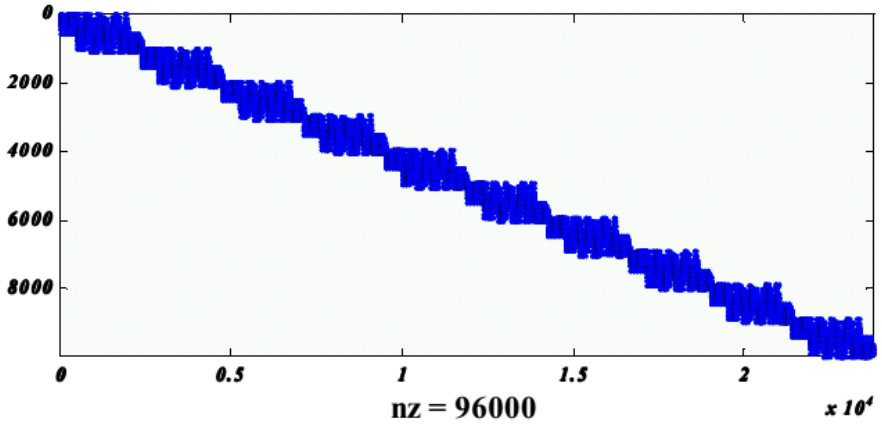

(d)

Fig. 9 Pattern of equilibrium matrix of example 1, (a) Linear element, (b) Quadratic element, (c) Cubic element, (d) Quartic element

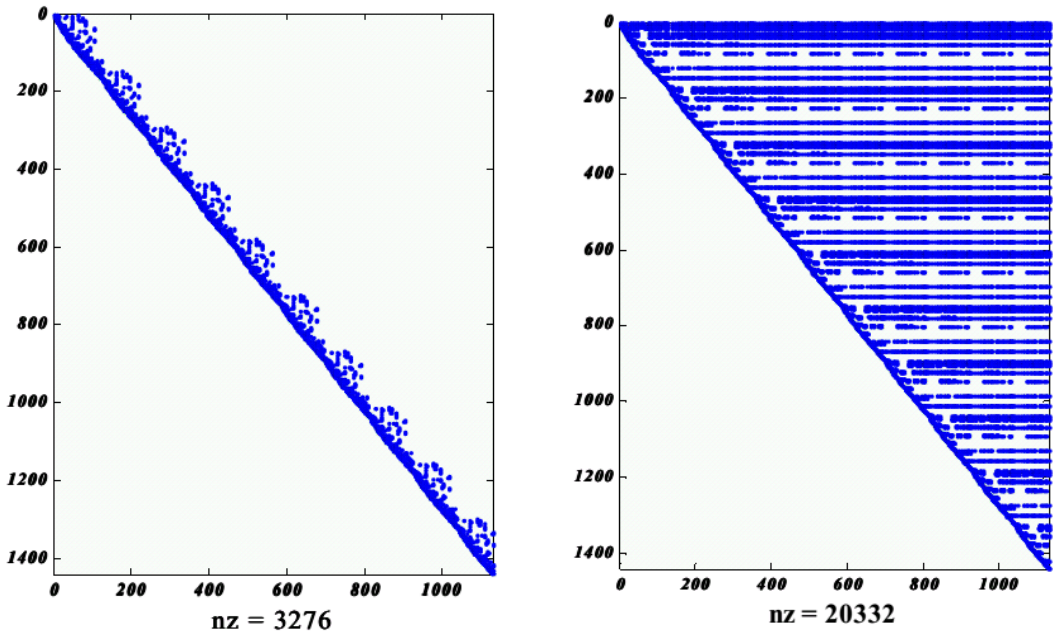

Graph Theoretical LU Factorization

(a)

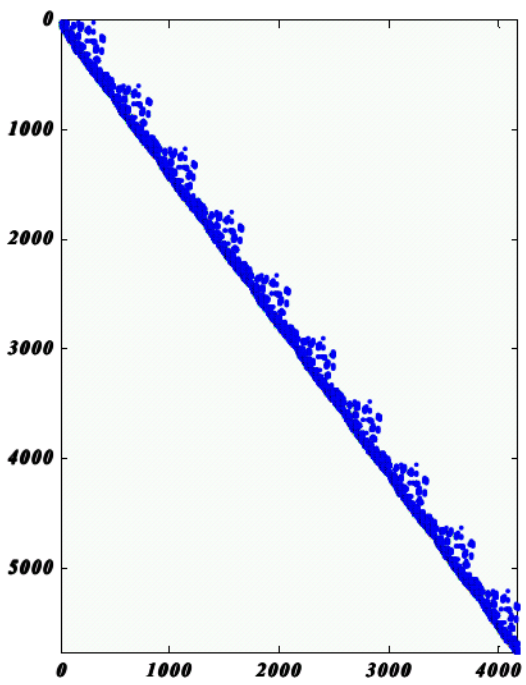

Graph Theoretical

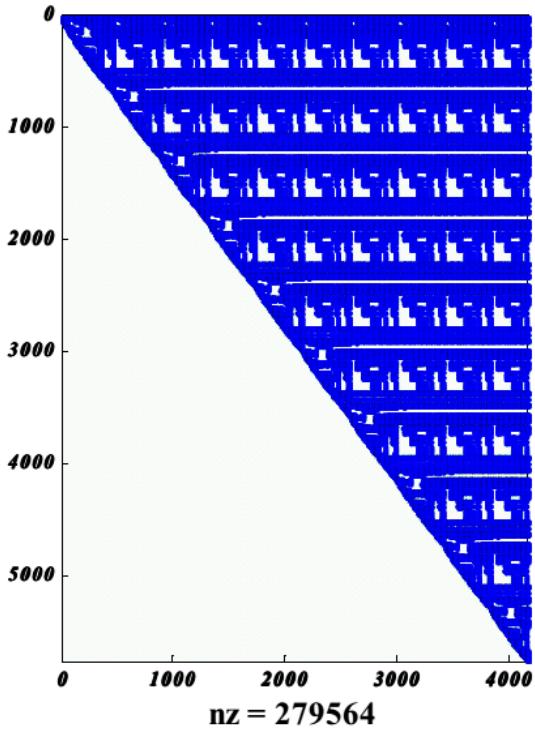

LU Factorization

(b)

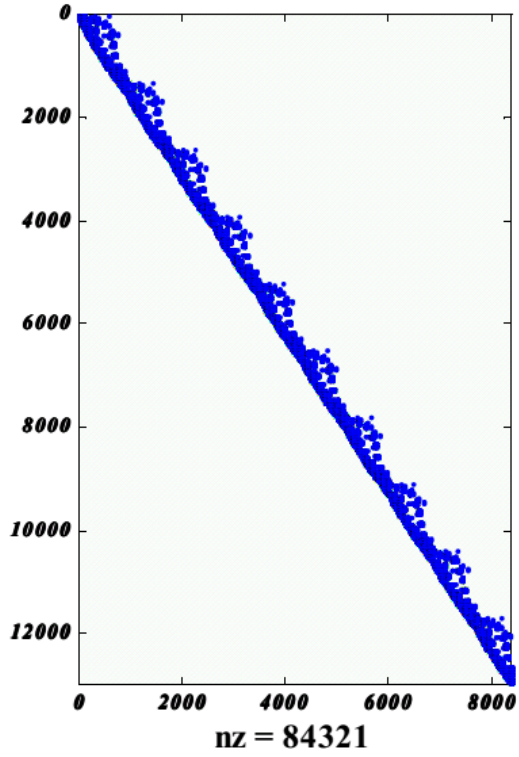

Graph Theoretical

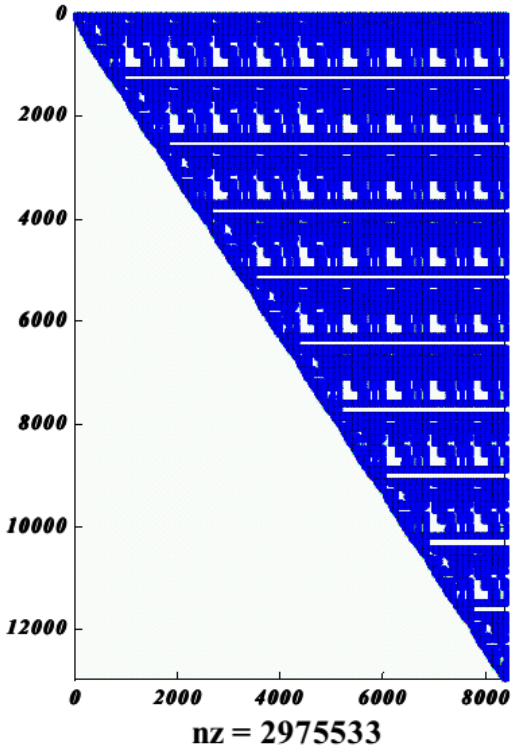

LU Factorization

(c)

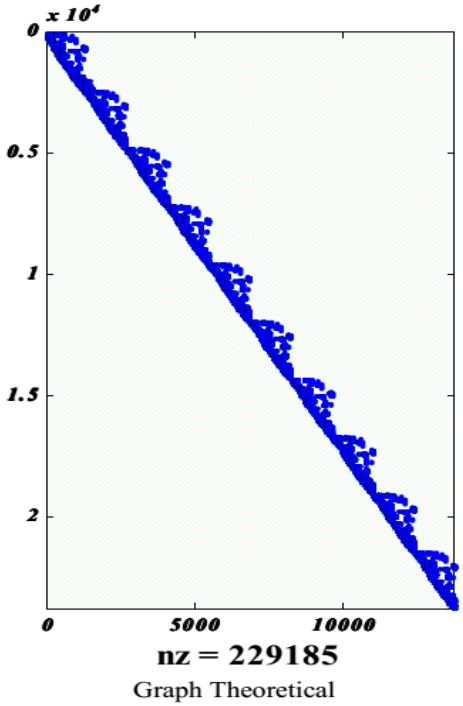

Could not be calculated

Graph Theoretical LU Factorization

(d)

Fig. 10 Pattern of null basis matrix of example 1, a) Linear element, b) Quadratic element, c) Cubic element, d) Quartic element

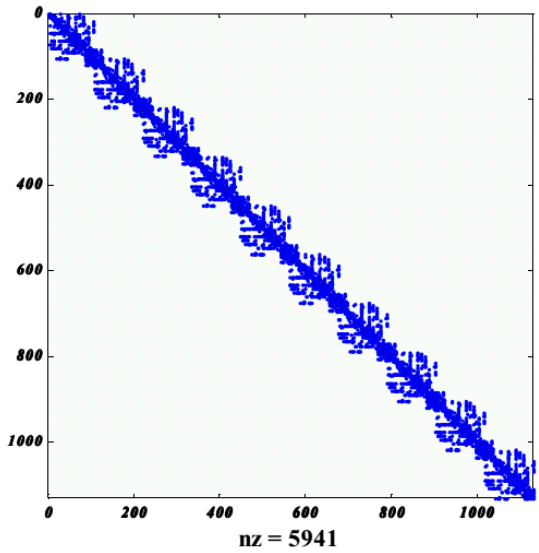

(a)

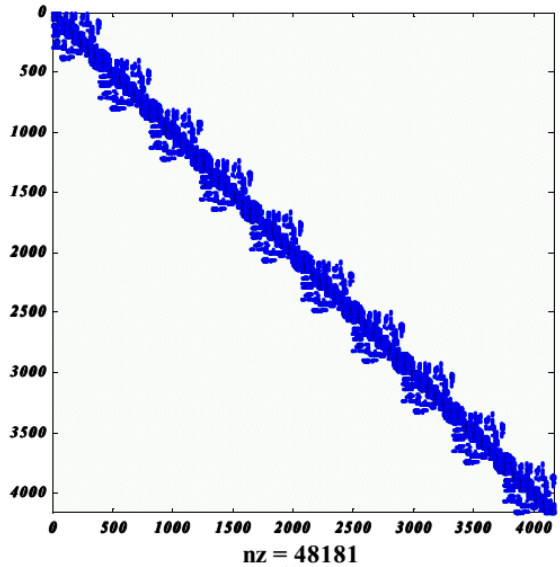

(b)

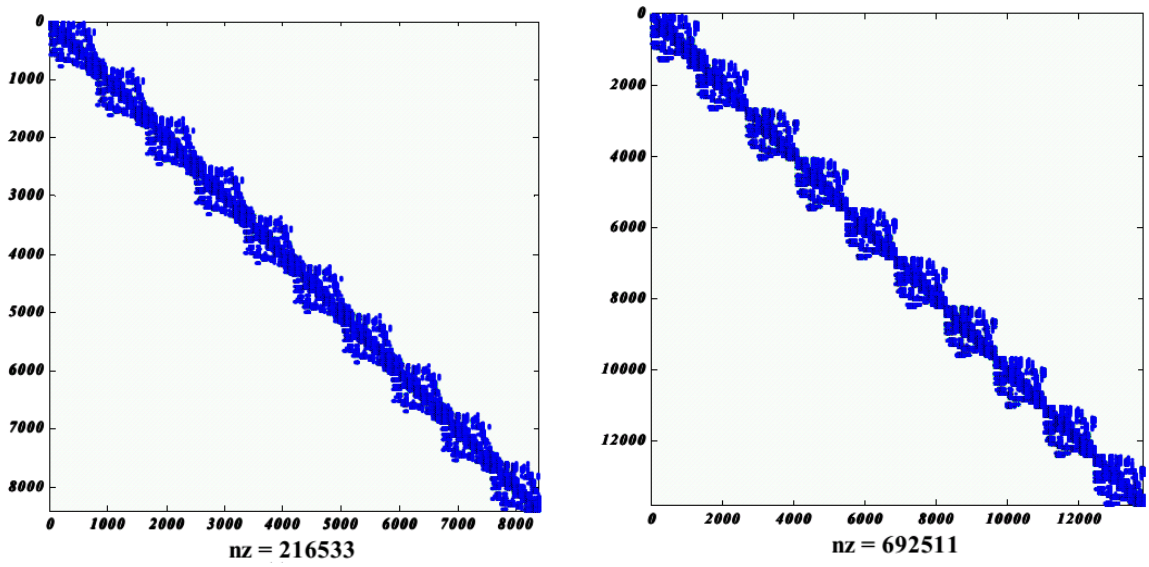

(c) (d)

Fig. 11 Pattern of flexibility matrix $B_l^t B_l$ using present method for example 1, a) Linear element, b) Quadratic element, c) Cubic element, d) Quartic element

Table 5 The comparison between present method and LU factorization method for Example 1

Element	$\frac{Time_{present\ method}}{Time_{LU\ method}}$	$\frac{nz(B_{l\ present\ method})}{nz(B_{l\ LU\ method})}$	$\frac{\lambda_{max}}{\lambda_{min}}(B_l^t \times B_l)$		$\max\lvert A \times B_l \rvert$	
			present method	LU method	present method	LU method
Linear	0.57	0.161	4.61e+4	3.45e+5	2.22e-16	1.38e-14
Quadratic	0.16	0.074	2.23e+5	8.45e+6	1.33e-15	5.54e-13
Cubic	0.01	0.028	4.96e+5	2.64e+7	1.13e-14	9.44e-12
Quartic	-	-	4.53e+4	-	7.25e-14	-

Example 2.

A thick wall structure is depicted in Fig. 12. The natural associate graph of FEM is illustrated in Fig. 13.This structure is discretized using 504 tetrahedron finite elements. The properties of the model are as follows:

Number of tetrahedron elements, M = 504 Elastic modulus, E = 2e+7 kN/m2 Poisson's ratio , ν = 0.2		
Number of nodes, N	Linear 195	Quadratic 1,053
DSI	2,445	8,943
Number of type I SESs	2,166	6,888
Number of type II SESs	0	1,776
Number of type III SESs	279	279

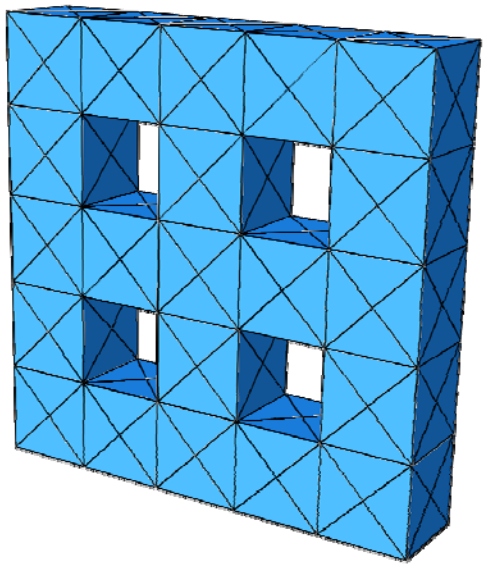

Fig. 12 A thick wall structure

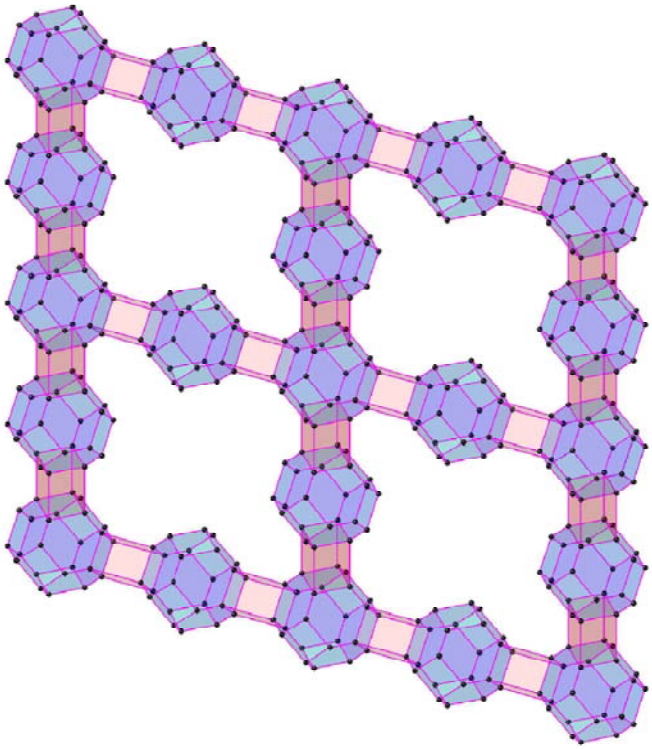

Fig. 13 Natural associate graph of FEM for thick wall structure of example 2.

The pattern of equilibrium matrix is shown in Fig. 14 for linear and quadratic elements. The pattern of the final null basis obtained by the present method and LU factorization method are depicted in Fig. 15. The flexibility matrix (G) is also well-structured as shown in Fig. 16. The comparison between present method and LU factorization method is prepared in Table 6.

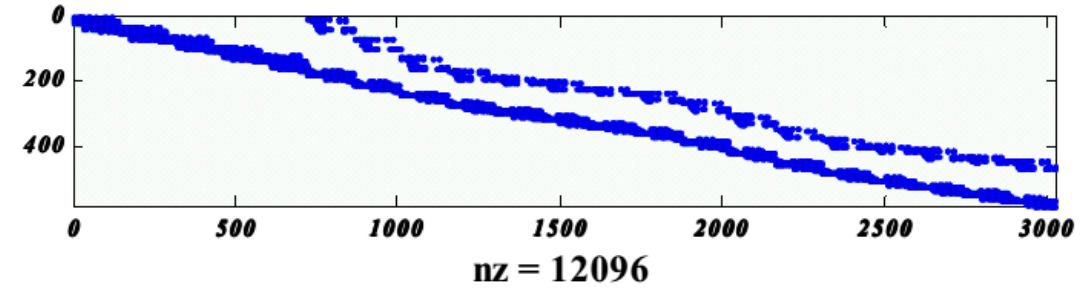

(a)

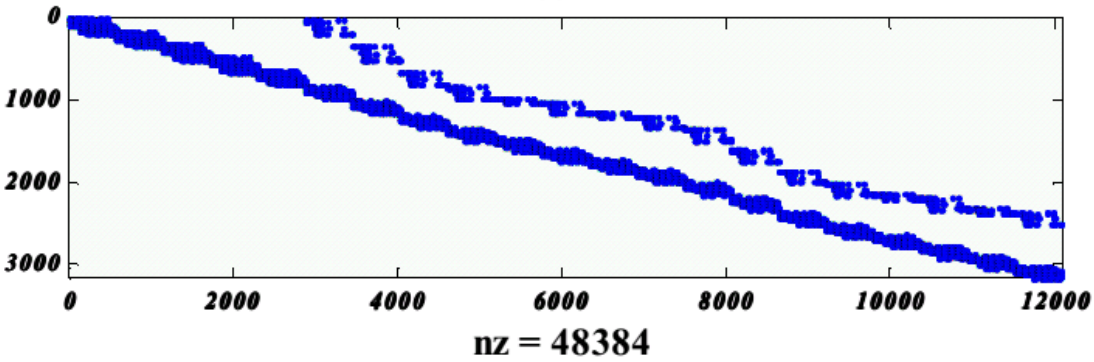

(b)

Fig. 14 Pattern of equilibrium matrix of example 2, a) Linear element, b) Quadratic element

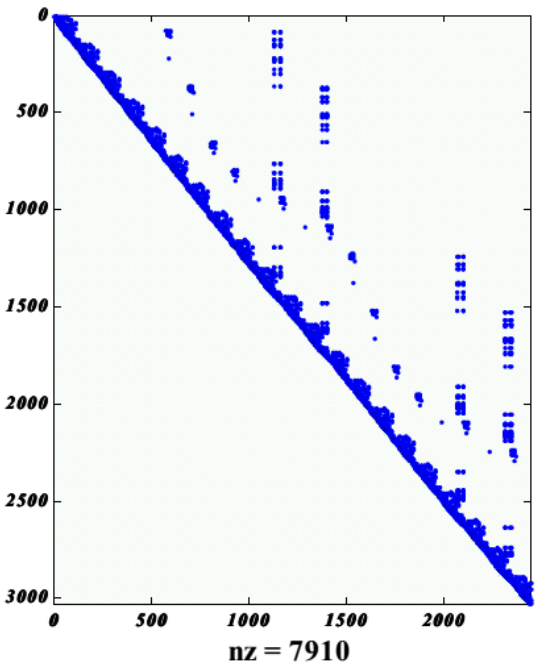

Graph Theoretical

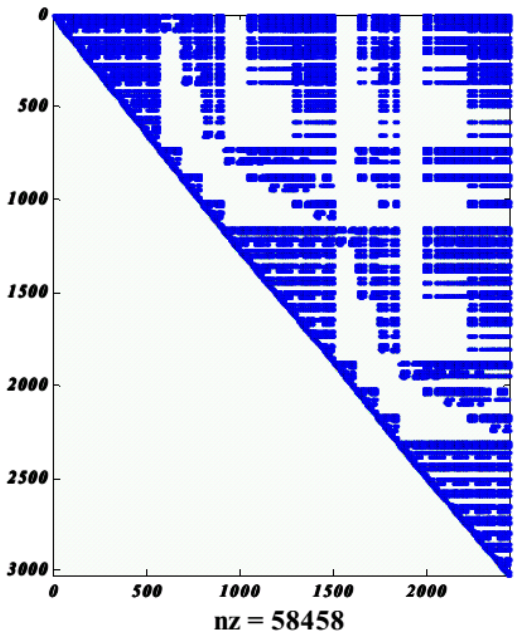

LU Factorization

(a)

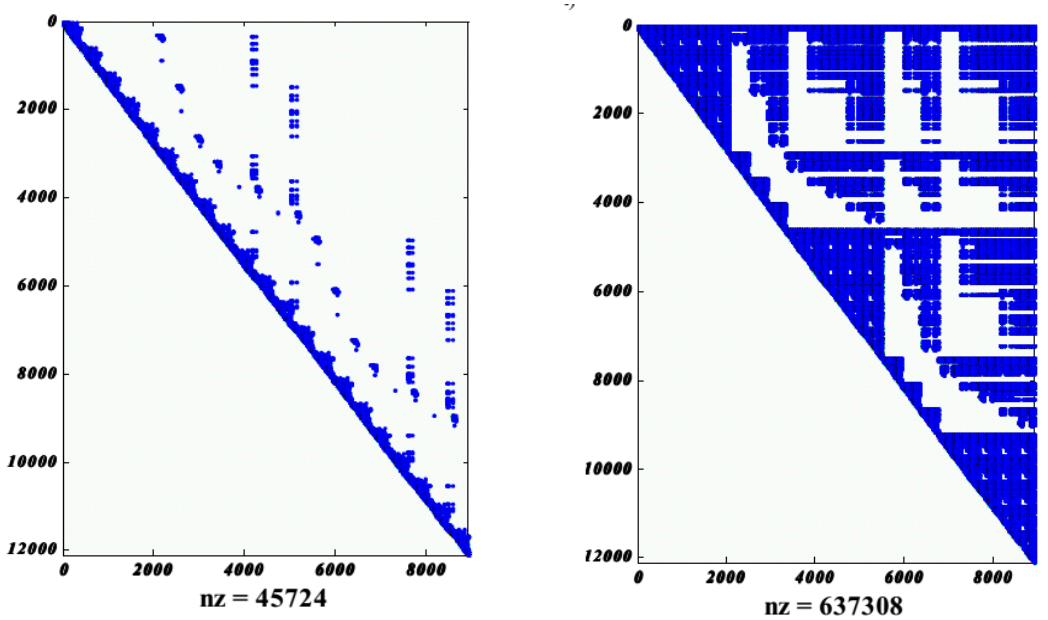

Graph Theoretical LU Factorization

(b)

Fig. 15 Pattern of null basis matrix of example 2, a) Linear element, b) Quadratic element

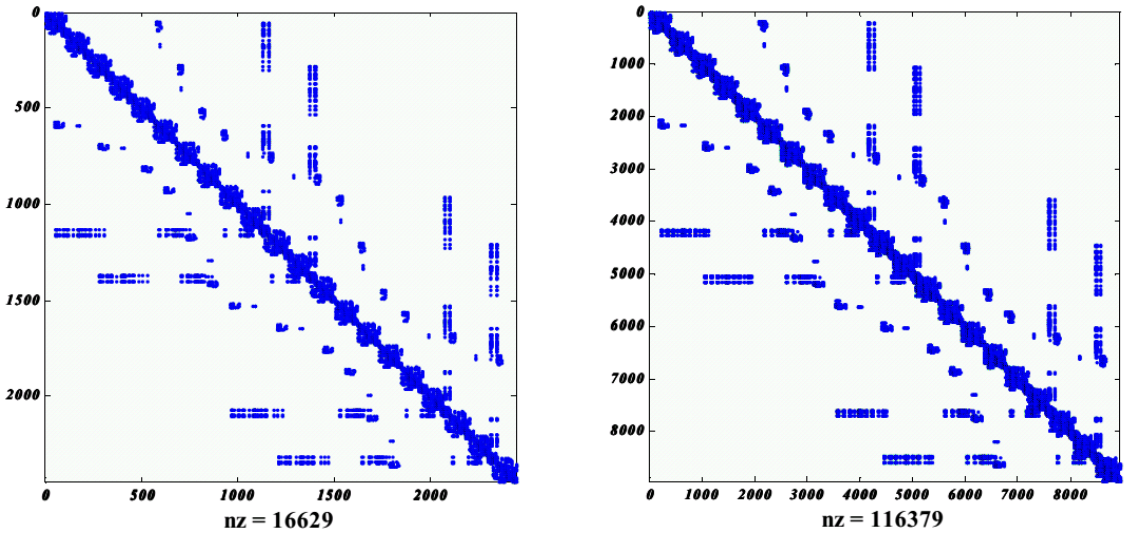

(a) (b)

Fig. 16 Pattern of flexibility matrix $B_1^t B_1$ using present method for example 2, a) Linear element, b) Quadratic element

Table 6 The comparison between present method and LU factorization method for example 2.

Element	$\frac{Time_{present\ method}}{Time_{LU\ method}}$	$\frac{nz(B_{1\ present\ method})}{nz(B_{1\ LU\ method})}$	$\frac{\lambda_{max}}{\lambda_{min}}(B_1^t \times B_1)$		$\max\lvert A \times B_1 \rvert$	
			present method	LU method	present method	LU method
Linear	0.38	0.135	5.50e+5	5.52e+5	4.77e-15	2.81e-13
Quadratic	0.09	0.072	2.15e+6	2.30e+7	2.05e-14	2.84e-12

Finally the present method is validated through comparison of nodal displacements using the present graph-theoretical force method and the displacement method. Six concentrated forces are applied at the six nodes of wall and the structure is supported in a statically determinate fashion as shown in Fig. 17. The amount of P is 10 kN and the dimension wall is $5^m \times 1^m \times 5^m$. The results are verified by standard displacement method in Table 7.

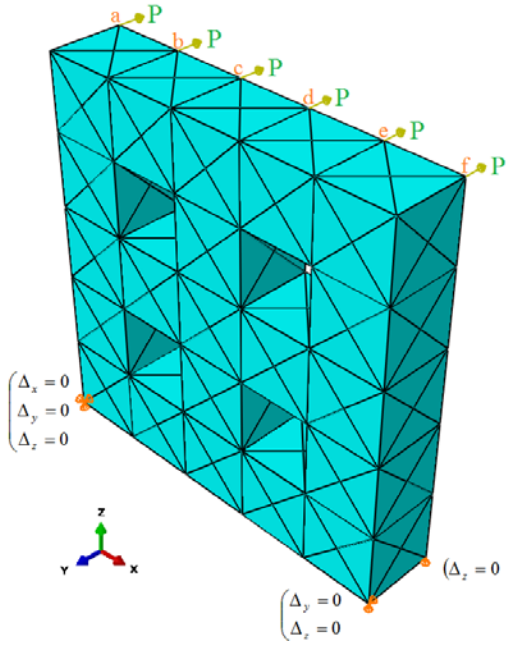

Fig. 17 The applied loads and boundary condition of thick wall structure

Table 7 Comparison between nodal displacements obtained by proposed force method and displacement method

	Node label		a	b	c	d	e	f
Displacement method	u_x (m)	Linear	-0.000101605	-0.000101470	-0.000100347	-0.000099177	-0.000098720	-0.000099067
		Quadratic	-0.000282728	-0.000283972	-0.000281390	-0.000278939	-0.000277491	-0.000279518
	u_y (m)	Linear	-0.001332250	-0.001288580	-0.001242980	-0.001195120	-0.001145740	-0.001097410
		Quadratic	-0.003451220	-0.003358890	-0.003264150	-0.003164890	-0.003061760	-0.002962390
	u_z (m)	Linear	-0.000263179	-0.000237067	-0.000210461	-0.000184183	-0.000158512	-0.000133218
		Quadratic	-0.000685347	-0.000616882	-0.000546970	-0.000478096	-0.000409829	-0.000343088
Proposed force method	u_x (m)	Linear	-0.000101630	-0.000101529	-0.000100406	-0.000099233	-0.000098740	-0.000099139
		Quadratic	-0.000282791	-0.000283962	-0.000281393	-0.000278857	-0.000277576	-0.000279610
	u_y (m)	Linear	-0.001332298	-0.001288607	-0.001242986	-0.001195163	-0.001145798	-0.001097509
		Quadratic	-0.003451272	-0.003358832	-0.003264242	-0.003164890	-0.003061837	-0.002962488
	u_z (m)	Linear	-0.000263085	-0.000237063	-0.000210526	-0.000184163	-0.000158535	-0.000133224
		Quadratic	-0.000685341	-0.000616803	-0.000546978	-0.000478170	-0.000409729	-0.000343107

Conclusions

The main conclusions of this paper are as follows:

Solution of many examples reveals that good accuracy can be achieved by the present algorithm as shown in Tables 5 and 6.

- Flexibility matrices obtained are highly sparse with narrowly banded. This is due to the use of regional cycles of the natural associate graphs and appropriate ordering of the selected self-equilibrating systems.
- The conditioning of the flexibility matrices generated by the present algorithm is better than those formed by the LU method, as illustrated is Tables 5 and 6.
- Due to a high reduction in the number of floating point operations, the resulted null basis has better accuracy

in comparison to other methods. This is obvious, since more than 65% of the null vectors are selected without numerical analysis and the remaining null vectors are obtained with working on small and limited lists.

- The required computational time for the present method is considerably lower than those of the algebraic methods. Since the complexity of the LU method is $O(n^3)$, if the DSI of the model increases, then the time difference dramatically rises. Here, $O(n^3)$ shows that the algorithm has order of n^3 time complexity**,** with n being the size of the problem**.**
- In the present method, numbering the nodes of a finite element model is less important and only a suitable ordering of the members of the natural associate graph is required for reducing the bandwidth of the flexibility matrices.
- The method developed in this paper can easily be extended to the analysis of FEMs containing other types of elements.
- Though no symmety is utilized in this paper, however, one can use symmetry in the force method similar to the displacement approach [29-31].

Acknowledgement: The first author is grateful to the Iran National Science Foundation for the support.

References

[1] Henderson JC de C. Topological aspects of structural analysis, Aircraft Engineering and Aerospace Technology, 1960, Vol. 32, pp. 137–141.

[2] Maunder EAW. Topological and Linear Analysis of Skeletal Structures, Ph.D. Thesis, London University, Imperial College, 1971.

[3] Henderson JC de C, Maunder EAW. A problem in applied topology: on the selection of cycles for the flexibility analysis of skeletal structures, IMA Journal of Applied Mathematics, 1969, Vol. 5, pp. 254–269.

[4] Kaveh A. Application of Topology and Matroid Theory to the Analysis of Structures, Ph.D. Thesis, London University, Imperial College, 1974.

[5] Kaveh A. An efficient flexibility analysis of structures, Computers & Structures, 1986, Vol. 22, pp. 973-977.

[6] Kaveh A. A combinatorial optimization problem Optimal generalized cycle bases, Computer Methods in Applied Mechanics and Engineering, 1979, Vol. 20, pp. 39–52.

[7] Cassell AC. An alternative method for finite element analysis; a combinatorial approach to the flexibility method, Proc. Royal Soc. London, 1976, Vol. A 352, pp. 73–89.

[8] Denke PH. A General Digital Computer Analysis of Statically Indeterminate Structures, NASA-TD-D-1666, 1962.

[9] Robinson J. Integrated Theory of Finite Element Methods, Wiley, New York, 1973.

[10] Topcu A. A Contribution to the Systematic Analysis of Finite Element Structures Using the Force Method, (in German) Doctoral Dissertation, Essen University, 1979.

[11] Kaneko I, Lawo M, Thierauf G. On computational procedures for the force methods, International Journal for Numerical Methods in Engineering, 1982, Vol. 18, pp. 1469–1495.

[12] Soyer E, Topçu A. Sparse self-stress matrices for the finite element force method, International Journal for Numerical Methods in Engineering, 2001, Vol. 50, pp. 2175–2194.

[13] Gilbert JR, Heath MT. Computing a sparse basis for the nullspace, SIAM Journal on Algebraic Discrete Methods, 1987, Vol. 8, pp. 446–459.

[14] Coleman TF, Pothen A. The null space problem I; complexity, SIAM Journal on Algebraic Discrete Methods, 1986, Vol. 7, pp. 527–537.

[15] Coleman TF, Pothen A. The null space problem II; algorithms, SIAM Journal on Algebraic Discrete Methods, 1987, Vol. 8, pp. 544–561.

[16] Pothen A. Sparse null basis computation in structural optimization, Numerische Mathematik, 1989, Vol. 55, pp. 501–519.

[17] Heath MT, Plemmons R, Ward J. Sparse orthogonal schemes for structural optimization using the force method, SIAM Journal on Scientific and Statistical Computing, 1984, Vol. 5, pp. 514–532.

[18] Patnaik SN. An integrated force method for discrete analysis, International Journal for Numerical Methods in Engineering, 1973, Vol. 6, pp. 237–251.

[19] Patnaik SN, Berke L, Gallagher RH. Integrated force method versus displacement method for finite element analysis, Computers & Structures, 1991, Vol. 38, pp. 377–407.

[20] Kaveh A, Massoudi MS. Efficient finite element analysis by graph-theoretical force method; rectangular and triangular plate bending elements, Scientia Iranica, 2011, Vol. 18, pp. 1045–1053.

[21] Kaveh A, Koohestani K. Efficient graph-theoretical force method for three dimensional finite element analysis. Commun, Communications in Numerical Methods in Engineering, 2008, Vol. 24, pp. 1533–1551.

[22] Kaveh A, Tolou Kian MJ. Efficient finite element analysis using graph-theoretical force method with brick elements, Finite Elements in Analysis and Design, 2012, Vol. 54, pp. 1–15.

[23] Kaveh A, Tolou Kian MJ. Efficient finite element analysis of models comprised of higher order triangular elements, Acta Mechanica, 2013, Vol. 224, pp. 1957-1975.

[24] Kaveh A, Massoudi MS, Massoudi MJ. Efficient finite element analysis using graph-theoretical force method; hexahedron elements, Computers & Structures, 2013, Vol. 128, pp. 175–188.

[25] Kaveh A. Computaional Structural Analysis and Finite Element Methods, Springer Verlag, GmbH, Wien-NewYork, 2014.

[26] Kaveh A, Naseri Nasab E. A new four-node quadrilateral plate bending element for highly sparse and banded flexibility matrices, Acta Mechanica, 2010, Vol. 209, pp. 295–309.

[27] Przemieniecki JS. Theory of Matrix Structural Analysis, McGraw-Hill, New York, 1968.

[28] Kaveh A. Graphs and structures, Computers & Structures, 1991, Vol. 40, pp. 893-901**.**

[29] Kaveh A. Optimal Structural Analysis Using Concepts of Symmetry and Regularity, Springer Verlag, Wien, 2013.

[30] Kaveh A. Rahami H. An efficient method for decomposition of regular structures using graph products, International journal for numerical methods in engineering, 2004, Vol. 61, pp. 1797-1808.

[31] Kaveh A, Salimbahrami B. Eigensolution of symmetric frames using graph factorization, Communications in Numerical Methods in Engineering, 2004, Vol. 20, pp. 889-910.